ISSN 0023-1584, Kinetics and Catalysis, 2008, Vol. 49, No. 3, pp. 344–351. © MAIK "Nauka/Interperiodica" (Russia), 2008.
Original Russian Text © N.M. Rubtsov, G.I. Tsvetkov, V.I. Chernysh, 2008, published in Kinetika i Kataliz, 2008, Vol. 49, No. 3, pp. 363–371.

Different Effects of Active Minor Admixtures on Hydrogen and Methane Ignitions

N. M. Rubtsov, G. I. Tsvetkov, and V. I. Chernysh

Institute of Structural Macrokinetics and Materials Research Problems, Russian Academy of Sciences, Chernogolovka, Moscow oblast, 142432 Russia

e-mail: nmrubtss@mtu-net.ru

Received May 2, 2007

Abstract—The methane combustion inhibitor CCl_4 exerts no effect on the first ignition limit of hydrogen; therefore, the role of hydrogen atoms in hydrocarbon oxidation consists at least of participating in longer reaction chains than are observed in hydrogen oxidation. The upper limits of the rate constants of the reactions of hydrogen atoms with propylene and isobutylene molecules were estimated by the self-ignition limit method to be $(1.0 \pm 0.3) \times 10^{-11}\exp(-1450 \pm 400/T)$ and $(0.8 \pm 0.3) \times 10^{-11}\exp(-550 \pm 200/T)$ cm^3 $molecule^{-1}$ s^{-1}, respectively, in the temperature range of 840–950 K. These data are evidence that the stronger inductive effect of the two methyl groups in isobutylene lowers the energy barrier to the H + *iso*-C_4H_8 reaction. It has been demonstrated experimentally that chemiluminescence in the hydrocarbon flame front at atmospheric pressure precedes heat evolution. Throughout the pressure and temperature ranges examined (5–750 Torr, 298–950 K), the chain mechanism determines the basic laws of combustion.

DOI: 10.1134/S002315840803004X

The problem of ensuring the explosion safety of hydrogen–air and methane–air mixtures is among the technological challenges in hydrogen and fossil-fuel power engineering. It was demonstrated (see, e.g., [1–4]) that the rates of gas-phase ignition, combustion, explosion, and detonation are determined by the competition between chain branching and termination reactions and that self-heating is a consequence of chain combustion. Nevertheless, one can find new publications in which the chain character of combustion is neglected. Until recently, the role of the branched-chain mechanism has been denied for pressures above a few tens of torrs (see, e.g., [5–7]). This denial is often based on the agreement between experimental data and calculations entirely neglecting the branched-chain mechanism (see, e.g., [8–10]). However, this agreement is observed when the real H_2 and CO oxidation processes are replaced with overall reactions involving only the starting and final substances. Kislov et al. [9] assign some parameters called rate constants to these overall reactions and claim that the calculated and experimental data are in good agreement. These parameters are derived from data obtained for one process under the groundless assumption that this process consists of a single step. However, it is well known that H_2 and CO oxidations are not single-step processes, contrary to the views presented in [8, 9], and, therefore, any agreement between calculated and experimental data is out of the question. In some works (see, e.g., [11, Table 1, 12]), numerical calculations for the kinetic mechanism of combustion are used to derive effective values of the preexponential factor and activation energy for a first-order reaction in Arrhenius form and these values are used to describe the process. However, the resulting equation is absolutely inapplicable to branched-chain processes [1] because the real process is again replaced with an imaginary reaction. Kostenko et al. [11, 12] suggest finding the ignition conditions for a gas mixture by determining the temperature at which the heat generation rate is equal to the heat dissipation rate, not by determining the conditions under which the chain branching rate is equal to the chain termination rate. Thus, Kostenko et al. [11, 12] try to explain the ignition conditions in terms of thermal theory, ignoring the established fact that the main features of gas ignition and combustion processes are determined by their branched-chain mechanism [1–4]. Taking into account the branched-chain character of gas-phase combustion processes enables one to interpret observations correctly and, moreover, to control these process using active admixtures.

For efficient use of chemical additions, it is necessary to know the detailed mechanism of combustion, including the rate constants of the elementary steps. This is essential from the standpoint of both combustion process control [13] and chemical conversion. For example, when studying the activity of unsaturated hydrocarbons as active admixtures, it should be expected that isobutylene ((CH_3)–$C(CH_3)$=CH_2), as compared to propylene (CH_3–CH=CH_2), will offer greater steric hindrance for approaching hydrogen atoms. At the same time, the energy barrier in the reaction between isobutylene and H must be lower owing to

the stronger inductive effect of the two methyl groups in isobutylene.

The purposes of this work are as follows:

(1) to establish a correlation between the inhibition efficiency and the specific features of the chain combustion mechanism by studying the effects of methane combustion inhibitors on hydrogen combustion and the effects of hydrogen combustion inhibitors on methane combustion by means of induction period and first ignition limit measurements for the stoichiometric mixtures $2H_2 + O_2$ and natural gas (NG) + $2O_2$ in the presence of small additions of C_3H_6, *iso*-C_4H_8, CCl_4, and SF_6;

(2) to estimate the preexponential factors and activation energies for the reactions of hydrogen atoms with C_3H_6 and *iso*-C_4H_8 molecules using the ignition limit method;

(3) to determine the time sequence of self-heating and luminescence in the flame front by studying the initiated ignition of a natural gas + air mixture at atmospheric pressure.

EXPERIMENTAL

Experiments were carried out using a static vacuum technique [14] in three types of reactors. Reactor I, which was used at pressures of 5–35 Torr and temperatures of 845–973 K, was a furnace-heated quartz cylinder 3.6 cm in diameter and 25 cm in length. The furnace temperature was set using a KVA-501 temperature regulator with an accuracy of ±0.5 K. A thin chromel/alumel thermocouple 40 μm in diameter was moved along the reactor axis in order to evaluate the uniformity of the temperature distribution in the reactor, which was found to be ±0.5 K at 900 K. The reactor and the furnace had an optical quartz window at one end. Stoichiometric mixtures of hydrogen and NG with oxygen were examined. Kinetic measurements at 1 atm and 298 K for the initiated ignition of NG + air mixtures were carried out in reactor II, which was a stainless steel cylinder 10 cm in diameter and 20 cm in length, and in reactor III, which was a a horizontal quartz tube 4 cm in diameter and 100 cm in length. Combustion was initiated with a spark (0.91 J) in the reactor center (reactor II) or at a reactor end (reactor III). The opposite end of reactor III was sealed. The initial temperature was 293 K. Integral luminescence in reactor II was monitored through an end-face optical window of diameter 3.5 cm using an FEU-71 photomultiplier (spectral sensitivity range of 200–600 nm). Gas pressure was monitored with a piezoelectric sensor. The signals from the photomultiplier and the pressure sensor were directed to an S9-16 dual-trace memory oscilloscope. Reactor III was equipped with a collimator 0.5 mm in diameter and 10 cm in length, which was mounted perpendicularly to the reactor surface at a distance of 80 cm from the initiation point. A thin chromel/alumel thermocouple 40 μm in diameter was placed at the reactor axis at precisely the same distance from the initiation point. The collimator hole was sighted at the thermojunction. Diethyl ether (0.25 cm^3) was sprayed in reactor III, both ends of the reactor were sealed, and the mixture was left to homogenize for 10 min. Thereafter, one end of the reactor was sealed and combustion was initiated. After initiation, the propagating flame reached the thermocouple and was simultaneously detected in the collimator hole using either an FEU-39 photomultiplier (fitted with a 435 ± 5 nm interference filter) or an FR-611 photoresistor (PbSe element, sensitivity range of 0.6–4.4 μm). Light emission was registered in the spectral range of 3.4–3.8 μm. Light with $\lambda < 3.4$ μm was cut off using an InAs filter, and $\lambda = 3.8$ μm is the transmission cutoff of quartz. The photoresistor FR-611 was fitted with a resonance preamplifier, whose signal was directed to a U2-8 selective amplifier. The signal from the amplifier U2-8 was directed to an S9-16 oscilloscope. The oscilloscope recorded a variable signal, whose envelope was the kinetic profile of IR radiation.

In the case of self-ignition, we recorded the emission from the electronically excited OH^* radicals ($A^2\Sigma^+$) at $\lambda = 306$ nm using an interference filter ($\Delta\lambda = 25$ nm) and an FEU-71 photomultiplier. The signal from the photomultiplier was directed to one of the inputs of an S9-16 dual-trace memory oscilloscope operating in the leading mode. The synchronization input of the oscilloscope received the signal from the optocoupler used to detect the instant the gas admission assembly and let the combustible mixture into the vacuumized reactor. This enabled us to measure induction periods and ignition delays (see below).

The first ignition limit P_1 was determined by the bleed-off method [5]. Experiments on $2H_2 + O_2$ mixtures containing admixtures were done in a reactor coated with magnesium oxide, and experiments on NG + $2O_2$ mixtures were performed over a quartz surface. According to gas chromatography data, NG contained 98% methane and 2% (propane + butane). H_2, O_2, C_3H_6, *iso*-C_4H_8, $(C_2H_5)_2O$, CO_2, and SF_6 were reagent-grade; CCl_4, $TiCl_4$, and MgO were extrapure-grade.

RESULTS AND DISCUSSION

Determination of the Rate Constants of the Reactions of Hydrogen Atoms with C_3H_6 and iso-C_4H_8 Molecules by the Ignition Limit Method

A convenient way of investigating combustion in the presence of active admixtures is by doing it under isothermal conditions near the first ignition limit, using the ignition limit method to determine the rate constants at combustion temperatures [15]. The low pressures corresponding to these conditions, at which trimolecular chain termination is negligible, allowed us to distinguish the inhibitor deactivating the active sites involved in chain propagation and the phlegmatizer effective in trimolecular chain termination. In this work, we measured P_1 and the self-ignition induction period (τ) in the

absence of an admixture (τ^0) and in the presence of an admixture (τ^{In}). In the strict sense, for inhibitor-containing mixtures we measured the ignition lag time τ_{lag}. This value is the sum of the ignition delay τ_{delay}, which is the time required for the mixture to come to the self-ignition region via inhibitor consumption, and the induction period τ^{In} itself:

$$\tau_{lag} = \tau_{delay} + \tau^{In}. \quad (1)$$

Since the duration of the reaction $H_2 + O_2$ is 5–50 ms and is much shorter than τ^0 (and τ^{In}), the τ_{lag} and τ^0 values were determined as the time interval between the mixture admission moment and the OH^* ($A^2\Sigma^+$) chemiluminescence intensity peak. For correct determination of P_1 under conditions such that inhibitor consumption can distort the measurements, it is necessary to take into account relationship (1). It was demonstrated [16] that, if the P_1 measurements are not distorted by inhibitor consumption, then, at a given ratio of the initial pressure to P_1, the true induction period τ^{In} for an inhibitor-containing mixture will be shorter than τ^0 for the inhibitor-free mixture. Therefore, the relationship $\tau^{In} < \tau^0$ at $P_0^{In}/P_1^{In} = P_0^0/P_1^0$, where P_1^0 is the first ignition limit in the absence of an inhibitor and P_0^{In} and P_0^0 are the initial self-ignition pressures in the presence and in the absence of the inhibitor [17], provides a criterion for checking that the observed first self-ignition limit P_1^{In} is undistorted. This criterion was used in this study when determining the first limit for inhibited self-ignition (hereafter, the first self-ignition limit in the presence and in the absence of an inhibitor is designated P_1).

Because the ignition limit method requires knowledge of the combustion mechanism, rate constants have mainly been determined for $H_2 + O_2$ (and $H_2 + CO + O_2$) flames in the presence of those small admixtures whose reactions are of interest. In these flames, the chain branching and termination rates are determined only by reactions of hydrogen atoms. Below, we will also consider chain termination on an inhibitor involving O atoms and OH^* radicals [18]. In the determination of the rate constants of homogeneous reactions by means of P_1 measurements, it is necessary to know the rate constants of the heterogeneous recombination of chain carriers, which can be derived with a high degree of accuracy from data obtained in the diffusion-controlled chain termination region. The recombination rate constant for a cylindrical reactor is $k_4 = 23.2\ D/d^2$, where D is the diffusion coefficient of the active site and d is the reactor diameter [19].

At temperatures well above the self-ignition peninsula cape temperature and pressures close to P_1, the mechanism of hydrogen combustion in the presence of an unsaturated hydrocarbon (e.g., *iso*-C_4H_8) can be represented as follows (the mean rate constants of the reactions presented below were used in the calculations):

$$H_2 + O_2 \longrightarrow 2OH^*,$$

$$k_0 = 0.32 \times 10^{-9} \times \exp(-21890/T)\ \text{cm}^3\ \text{molecule}^{-1}\ \text{s}^{-1}\ [20], \quad (0)$$

$$OH^* + H_2 \longrightarrow H_2O + H,$$

$$k_1 = 0.55 \times 10^{-11} \times \exp(-2000/T)\ \text{cm}^3\ \text{molecule}^{-1}\ \text{s}^{-1}\ [21], \quad (I)$$

$$H + O_2 \longrightarrow OH^* + O,$$

$$k_2 = 0.30 \times 10^{-9} \times \exp(-8379/T)\ \text{cm}^3\ \text{molecule}^{-1}\ \text{s}^{-1}\ [22], \quad (II)$$

$$O + H_2 \longrightarrow OH^* + H,$$

$$k_3 = 0.31 \times 10^{-9} \times \exp(-6900/T)\ \text{cm}^3\ \text{molecule}^{-1}\ \text{s}^{-1}\ [23], \quad (III)$$

$$H + \text{wall} \longrightarrow \text{termination}, \quad (IV)$$

$$H + iso\text{-}C_4H_8 \longrightarrow iso\text{-}C_4H_9^*, \quad (V)$$

$$O + iso\text{-}C_4H_8 \longrightarrow \text{products},$$

$$k_6 = 0.11 \times 10^{-10} \times \exp(128/T)\ \text{cm}^3\ \text{molecule}^{-1}\ \text{s}^{-1}\ [24], \quad (VI)$$

$$OH^* + iso\text{-}C_4H_8 \longrightarrow \text{products},$$

$$k_7 = 0.95 \times 10^{-11} \times \exp(503/T)\ \text{cm}^3\ \text{molecule}^{-1}\ \text{s}^{-1}\ [25], \quad (VII)$$

$$iso\text{-}C_4H_9^* + O_2 \longrightarrow iso\text{-}C_4H_8 + HO_2^*, \quad (VIII)$$

$$HO_2^* + \text{wall} \longrightarrow \text{termination}. \quad (IX)$$

In reaction (V), the hydrogen atom is added at the double bond to yield the unreactive radical *iso*-$C_4H_9^*$, which ensures chain termination via consecutive reactions (VIII) and (IX) [26]. The expression for P_1 based on the above mechanism can be reduced to the following form [18]:

$$[O_2]_{In} = \beta k_4/2k_2 + \beta k_5/2k_2[iso\text{-}C_4H_8]_{In}, \quad (2)$$

where $\beta = (1 + k_6[iso\text{-}C_4H_8]/k_3[H_2])(1 + k_7[iso\text{-}C_4H_8]/k_1[H_2])/(1 - k_6k_7[iso\text{-}C_4H_8]^2/k_3k_1[H_2]^2)$ and the concentration values correspond to P_1.

Taking into account the dependence of D on temperature, we will represent k_4 as

$$k_4 = 23.2(T/273)^n \times 760D^0/(Pd^2), \quad (3)$$

where D^0 is the diffusion coefficient for the mixture of the given composition at 760 Torr and 273 K, P is pressure (Torr), T is temperature, and n is between 1.5 and 1.8 and tends to 1.5 as the temperature is raised [27]. Replacing the concentrations with partial pressures and taking into account Eq. (3), we derive the following expression from Eq. (2):

$$PP_{O_2} = \beta(T/273)^{2.5}D^0 \times 10^{-19}/2k_2 + \beta k_5/2k_2 PP_{iso\text{-}C_4H_8}. \quad (4)$$

The temperature dependences of P_1 for detonating mixtures containing *iso*-C_4H_8 and C_3H_6 over the MgO surface are presented in Figs. 1a and 1b, respectively. Clearly, *iso*-C_4H_8 is a more effective inhibitor than propylene. As is shown in Figs. 1c and 1d, the data of the measurements at a constant temperature lie on straight lines in the PP_{O_2}–PP_{In} coordinates, indicating the constancy of the coefficient β under the measurement conditions examined. Since Eq. (4) is valid far from the cape of the self-ignition peninsula, we plotted data points for $P_1 < 12$ Torr in these coordinates, as was done in, e.g., [28]. The ordinate intercept, which is equal to $\beta(T/273)^{2.5}D^0 \times 10^{-19}/2k_2$, gives a k_2 value close to the known value [22] at $\beta = 1$. This may mean that reactions (VI) and (VII) do not cause chain termination, but are chain propagation reactions. From the ratios of the slopes of the straight lines in Figs. 1c and 1d to the free term of Eq. (4), we estimated the k_5 values, whose Arrhenius plots are presented in Figs. 1e and 1f. The activation energies and the preexponential factors of the rate constants were found to be equal to 4600 ± 1650 kJ/mol and $(0.8 \pm 0.3) \times 10^{-11}$ cm^3 molecule^{-1} s^{-1} for *iso*-C_4H_8 and 12 100 ± 3300 kJ/mol and $(1.0 \pm 0.3) \times 10^{-11}$ cm^3 molecule^{-1} s^{-1} for C_3H_6. Clearly, the energy barrier for the reaction between H and *iso*-C_4H_8 is lower owing to the stronger inductive effect of the two methyl groups. At the same time, the preexponential factor for this reaction is smaller because of the greater steric hindrance to the approaching hydrogen atoms. The fact that the characteristics of the process depend on the position of the π bond in the inhibitor molecule suggests that the chain avalanche plays a significant role in combustion. This dependence was observed for the first time in a study of the effect of C_3H_6 and *iso*-C_4H_8 on flame propagation in hydrogen-containing mixtures [13].

There has been a report in which the rate constants of the reactions of hydrogen atoms with the unsaturated hydrocarbons are larger than the corresponding values measured in this study and are equal to $0.6 \times 10^{-10}\exp(-849/T)$ cm^3 molecule^{-1} s^{-1} for *iso*-C_4H_8 and $0.22 \times 10^{-10}\exp(-785/T)$ cm^3 molecule^{-1} s^{-1} for C_3H_6 [29]. This discrepancy may arise from the fact that Harris and Pitts [29] used a different experimental procedure. They used a jet reactor containing an unsaturated hydrocarbon and methane as a source of hydrogen atoms and irradiated the mixture with a flash lamp [29]. The decline of the hydrogen atom concentration after a light pulse was monitored by the resonance fluorescence method. It was assumed in that study that hydrogen atoms result from methane decomposition under the action of a light pulse from the flash lamp and that the hydrocarbon reacts with the thus-generated H atoms. However, under these conditions, H atoms result from hydrocarbons as well and react with some mixture of intermediate species produced by photolysis. This can be responsible for the large values of the preexponential factors of the rate constants. Note that the substitution of the rate constants from [29] into Eq. (4) and P_1 calculation using the resulting equation suggest that the inhibitors shift the self-ignition region of the detonating mixture by more than 100 K to higher temperatures. This result is inconsistent with the available experimental data and indicates that the rate constants reported in [29] are overestimated. Very different values have been reported for the H + C_3H_6 reaction, which range between $1.3 \times 10^{13}\exp(-820/T)$ cm^3 molecule^{-1} s^{-1} [30] and $4.6 \times 10^{14}\exp(-2568/T)$ cm^3 molecule^{-1} s^{-1} [31]. Our value of the activation energy of this reaction is intermediate between these values.

For independent verification of our values of k_5 and $\beta = 1$, we calculated τ_{lag} values for mixtures containing an inhibitor (*iso*-C_4H_8) by solving the kinetic equations corresponding to mechanism (0)–(VII), which are unsteady-state with respect to the initial reactants and active sites, in the framework of the Cauchy problem. We used the eighth-order Runge–Kutta method, running the program package Maple 9.5. The $\tau_{lag} = \tau_{delay} + \tau^{In}$ value was taken to be equal to the time interval between the zero-time point and the H concentration peak. Figure 2 presents the calculated and experimental data for *iso*-C_4H_8. It is evident from Fig. 2 (compare the experimental data with calculated curve *1*) that the best agreement between the calculated and experimental data is observed for $\beta = 1$. Therefore, the reactions of H atoms and $OH^{\bullet}$ radicals with molecules of the unsaturated hydrocarbon possibly lead to chain propagation.

Thus, the branched-chain mechanism quantitatively determines the laws of hydrogen combustion, as is unequivocally indicated by the agreement between the experimental and theoretical data. It is clear from the above data that self-heating before ignition is negligible. Otherwise, there would have been no agreement between the experimental and theoretical data.

Self-ignition of Hydrogen and Natural Gas Mixtures with Oxygen in the Presence of Active Admixtures

Earlier, we demonstrated that chromium and molybdenum carbonyls, which inhibit the combustion of hydrocarbons (as was shown for C_3H_6 as an example), promote the combustion of hydrogen [32]. From this finding, we inferred that the role of hydrogen atoms in a chain unit is not limited to the reaction cycle (I)–(III). Propylene is an effective inhibitor of hydrogen combustion [2], and CCl_4 is regarded as a methane combustion

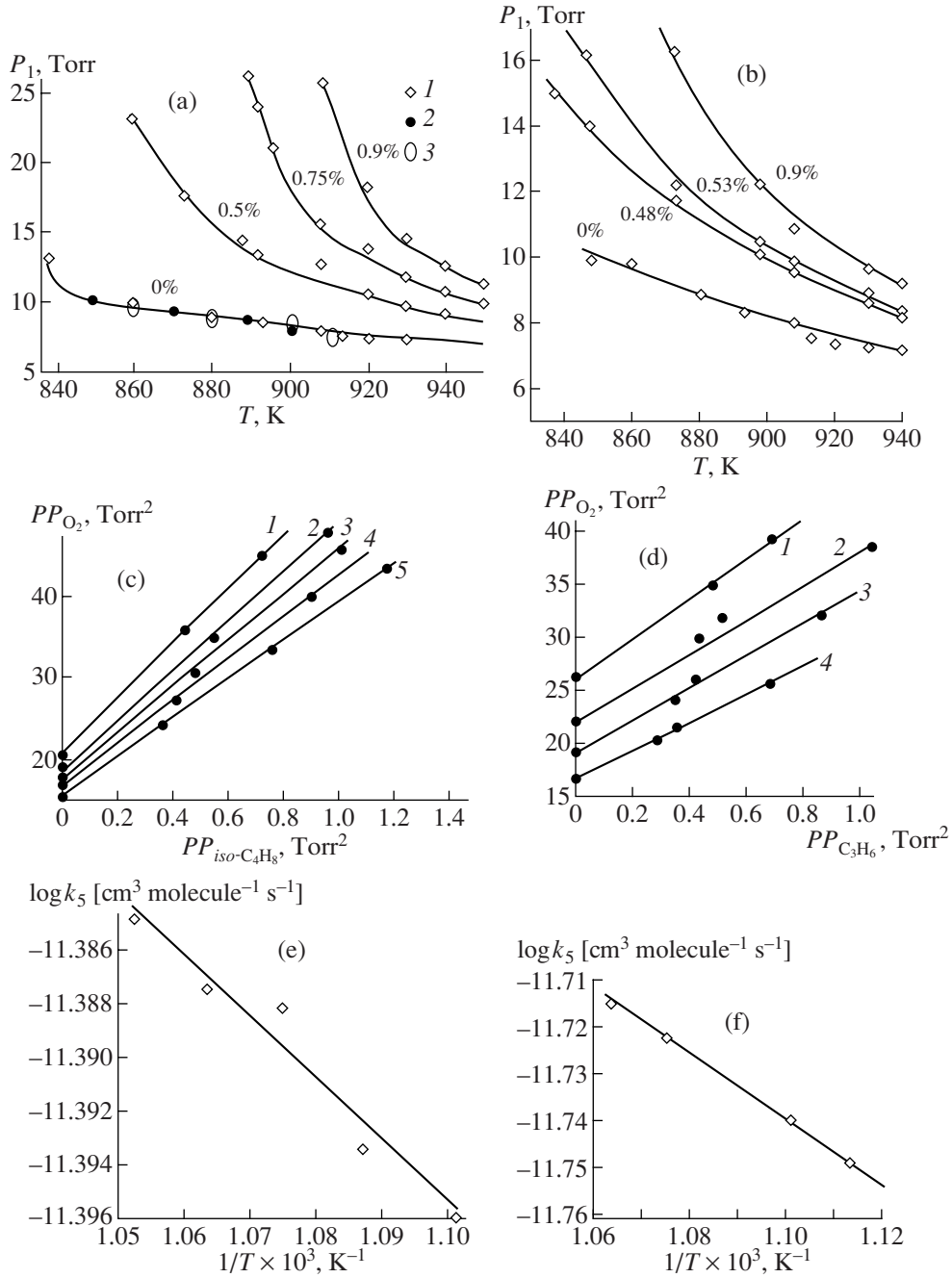

Fig. 1. Combustion of the detonating mixture over the MgO surface in the presence of C_3H_6, *iso*-C_4H_8, CCl_4, and SF_6: (a) temperature dependences of P_1 in the presence of (*1*) *iso*-C_4H_8, (*2*) CCl_4, and (*3*) SF_6 (the numbers at the curves are *iso*-C_4H_8 concentrations); (b) temperature dependences of P_1 in the presence of C_3H_6 (the propylene concentrations are indicated at the curves); (c) plot of Eq. (4) for *iso*-C_4H_8 at (*1*) 908, (*2*) 920, (*3*) 930, (*4*) 940, and (*5*) 950 K; (d) plot of Eq. (4) for C_3H_6 at (*1*) 896, (*2*) 910, (*3*) 930, and (*4*) 940 K; (e, f) $\log k_5$ versus $1/T$ for (e) *iso*-C_4H_8 and (f) C_3H_6.

inhibitor [33]. SF_6 admixtures reduce the second self-ignition limit for the reaction $H_2 + O_2$ [34], playing a significant role in the stabilization of the $HO_2^{\bullet}$ radical through the reaction $H + O_2 + SF_6 \longrightarrow HO_2^{\bullet} + SF_6^{V-V}$; that is, SF_6 is a combustion phlegmatizer. Carrying out the oxidation of H_2 and NG in the presence of these admixtures enabled us to verify the conclusions made in [32]. The stoichiometric methane + oxygen mixture self-ignites at higher temperatures than the detonating mixture because methane combustion is a less intensive process. Furthermore, the induction period in this process near P_1 is longer than 10 min [35]. This causes serious difficulties in P_1 measurements. For this reason,

in the study of the reaction NG + O_2 in the presence of an admixture, the induction period (or the ignition lag time) was measured at preset values of pressure and temperature. The τ^0 values for the NG + $2O_2$ mixtures were somewhat smaller than the same values measured for CH_4 + O_2 mixtures [35]. This discrepancy is due to the presence of more readily ignitable hydrocarbons in NG. Prior to the main experiments, we determined the lower concentration limit (LCL) of ignition in reactor II at 1 atm and 298 K, which was found to be (4.65 ± 0.05)%. This value was determined as the arithmetic mean between two NG concentrations in air such that initiated ignition was not observed for the lower one and was observed for the higher one. The LCL of NG appeared to be lower than the LCP of pure methane. This is in agreement with earlier data [5].

At 963 K, τ^0 for the NG + $2O_2$ mixture was reproducibly measured to be 22 ± 2 s. In the presence of 1% CCl_4, we measured τ_{lag} = 63 ± 5 s at 963 K. The fact that an ignition lag is observed experimentally means that the inhibitor (CCl_4 in this case) affects the rate of one of the steps of the chain unit of methane oxidation [36]. By contrast, in the presence of 2% SF_6, τ^{SF_6} = 21 ± 4 s; that is, $\tau^{SF_6} \approx \tau^0$. This indicates that SF_6 is not an inhibitor, but a combustion phlegmatizer involved in trimolecular chain termination. On the other hand, a 1% C_3H_6 admixture reduces the ignition lag $\tau^{C_3H_6}$ to 16 ± 4 s at the same temperature; that is, C_3H_6 is a promoter of methane combustion. Taking into account that propylene self-ignites more readily than methane [33] and that the LCL of NG is 0.5% lower than the LCL of CH_4 (because of the presence of higher hydrocarbons; see above), the latter inference is obvious.

The temperature dependences of P_1 for the detonating mixture over the MgO surface in the absence and in the presence of the above admixtures are plotted in Figs. 1a and 1b. Clearly, the unsaturated hydrocarbons exert a marked inhibiting effect on the ignition of the $2H_2$ + O_2 mixture. At the same time, neither CCl_4 nor SF_6 has an appreciable effect on P_1. The experimentally discovered opposite effects of the active admixtures C_3H_6 and CCl_4 on the self-ignition of hydrogen and NG suggest that hydrogen atoms do not play a crucial role in hydrocarbon oxidation, which is in agreement with our earlier results [32]. However, they are involved at least in longer reaction chains than are observed in hydrogen oxidation.

Note that, in the pressure range in which the above experiments were performed, the laws of gas combustion are determined by the chemical factor rather than by the thermal factor. The ignition of methane (and hydrogen above 20 Torr) is accompanied by a typical pop indicating that noticeable self-heating takes place. At the same time, experiments demonstrate that the combustion of the $2H_2$ + O_2 mixture (T = 860 K, P = 23 Torr, Fig. 1a) is completely suppressed at an inhibitor concentration of 0.5%, which is too low to change the thermophysical properties of the combustible mixture. This prompted us to perform a special-purpose study to elucidate the order in which self-heating and a chain avalanche take place in the flame front at atmospheric pressure.

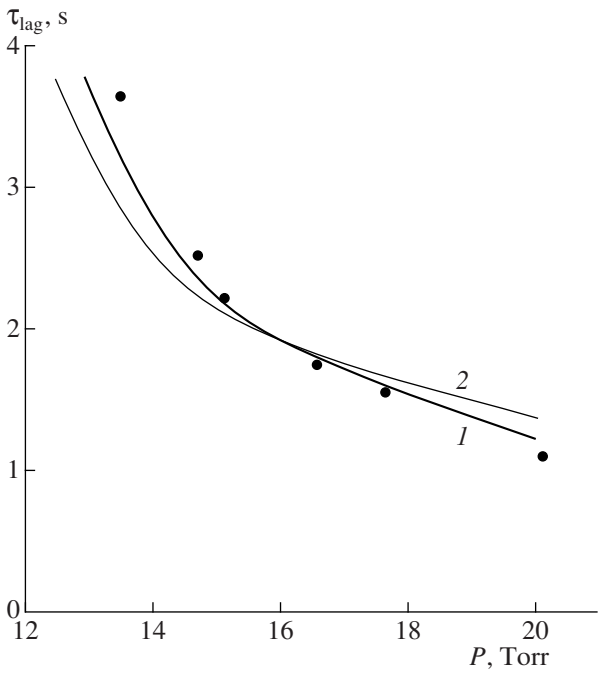

Fig. 2. Pressure dependences of the self-ignition lag time for the detonating mixture in the presence of 0.75% *iso*-C_4H_8 at 905 K. The points represent experimental data. The lines represent calculated data: (*1*) reactions (VI) and (VII) are ignored; (*2*) reactions (VI) and (VII) are taken into account.

The Determining Role of the Chain Mechanism in the Initiated Ignition of Natural Gas + Air and Diethyl Ether + Air Mixtures at Atmospheric Pressure

Metal carbonyls are known to be effective suppressants of hydrocarbon combustion [33]. However, these compounds are extremely toxic and, as a consequence, find only limited application [37]. Their inhibiting activity is attributed to the formation of highly reactive metal and metal oxide nanoparticles during combustion [32, 38]. In this study, we used a mixed inhibitor consisting of a metal chloride much less toxic than the carbonyls (specifically, $TiCl_4$) and CO_2. We demonstrate in Fig. 3 that a 0.4% $TiCl_4$ admixture reduces the natural gas oxidation rate (determined as the pressure or chemiluminescence increase rate) by a factor greater than 10. Thus, the very exothermic combustion process at atmospheric pressure can be inhibited by a small amount of the reactive admixture.

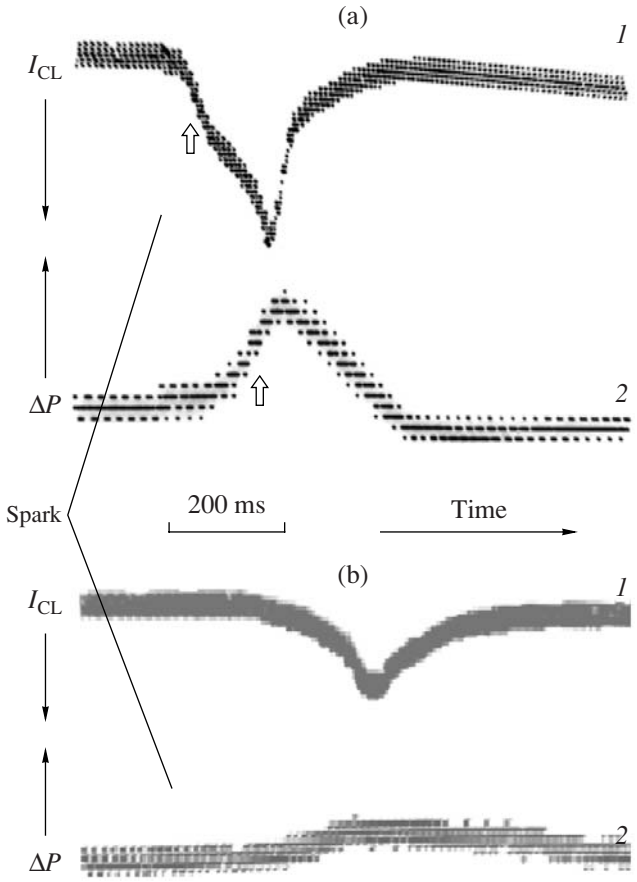

Fig. 3. Oscillograms characterizing the initiated ignition of natural gas in air: (a) 7.5% NG + 13% CO_2 + air, P = 1 atm, T = 298 K; (b) 7.5% NG + 13% CO_2 + 0.4% $TiCl_4$ + air, P = 1 atm, T = 298 K. (*1*) Time profile of chemiluminescence intensity. (b) Time profile of pressure.

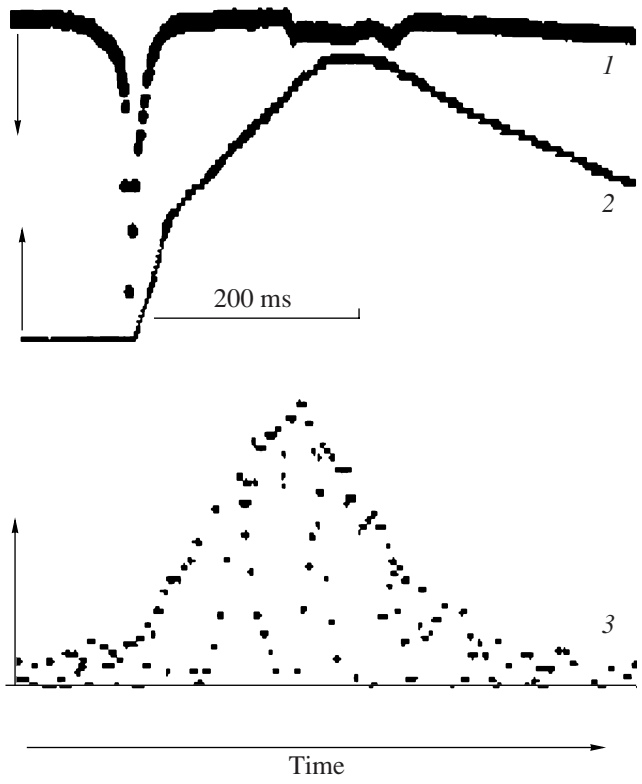

Fig. 4. Simultaneous oscillogram of (*1*) radiation from CH (λ = 431.5 nm), (*2*) temperature, and (*3*) IR radiation from H_2O (v = 1 region) for flame propagation in the reactor with an open end. P = 1 atm.

It is also clear from Fig. 3a that the chemiluminescence increase rate peak occurs 150 ms earlier than the pressure growth rate peak (these peaks are indicated by arrows). The pressure growth in initiated ignition is uniquely determined by the temperature growth because the number of moles is almost invariable throughout the reaction. Obviously, the temperature growth is a measure of reaction intensity. In our experiments, the pressure value reflected the average temperature of the gas mixture. Thus, it follows from Fig. 3a that the chain avalanche in combustion is developed definitely earlier than heat evolution begins. These data were verified by studying diethyl ether flame propagation in reactor III. Figure 4 presents the simultaneous oscillogram of λ = 431.5 nm radiation (CH, $A^2\Delta - X^2\Pi$ transition), temperature, and IR radiation in the region of the vibrational–rotational transition in H_2O (v = 1) measured at the reactor cross section 80 cm away from the ignition point. Clearly, the peak of CH radiation in the flame front occurs much earlier than both the temperature peak and the IR radiation peak (the latter also reflects the increase in heat evolution during combustion). The response time of a thermocouple 40 μm in diameter is ~25 ms [39], so the thermocouple inertia could not distort the measurements to any significant extent. Note that we compare the times at which the peaks of the above quantities occur, not the quantities themselves. Thus, for combustion in both a closed vessel and in a reactor open at one end, chemiluminescence is detected much earlier than self-heating. The data presented in Figs. 3 and 4 provide convincing evidence that the development of a chain avalanche precedes heat evolution in the flame front; that is, in agreement with earlier reports [1–4, 40], self-heating is a consequence of a developed chain reaction.

Thus, the upper limits of the rate constants of the reactions of hydrogen atoms with C_3H_6 and *iso*-C_4H_8 molecules have been estimated by the ignition limit method. The energy barrier in the H + *iso*-C_4H_8 reaction is lower owing to the stronger inductive effect of the methyl groups in the isobutylene molecule. At the same time, the preexponential factor for this reaction is smaller because of the greater steric hindrance for approaching hydrogen atoms. The methane combustion CCl_4 exerts no effect on the first limit of hydrogen ignition; that is, the role of hydrogen atoms in hydrocarbon oxidation likely consists of participating in longer reaction chains than are observed in hydrogen oxidation. By

the examples of natural gas and diethyl ether oxidation with air at atmospheric pressure, it has been demonstrated that the chain reaction mechanism determines the main laws of combustion. The chain avalanche precedes self-ignition. The fact that the chemical mechanism governs combustion both in the self-ignition regime and in the flame propagation regime does not allow one to represent the combustion process as a single-step reaction.

ACKNOWLEDGMENTS

This work was supported by the Russian Foundation for Basic Research (grant no. 02-03-32993a), CRDF (grant no. RUE1-2686-MO-05), and INTAS (grant no. 05-1000005-7664).

REFERENCES

1. Azatyan, V.V., *Zh. Fiz. Khim.*, 1999, vol. 73, no. 10, p. 1755 [*Russ. J. Phys. Chem.* (Engl. Transl.), vol. 78, no. 6, p. 1577].
2. Azatyan, V.V., Vagner, G.G., and Vedeshkin, G.K., *Zh. Fiz. Khim.*, 2004, vol. 78, no. 6, p. 1036 [*Russ. J. Phys. Chem.* (Engl. Transl.), vol. 78, no. 6, p. 896].
3. Azatyan, V.V., *Kinet. Katal.*, 1996, vol. 37, no. 4, p. 512 [*Kinet. Catal.* (Engl. Transl.), vol. 37, no. 4, p. 480].
4. Azatyan, V.V., Baklanov, D.I., Gvozdeva, L.G., et al., *Dokl. Akad. Nauk*, 2000, vol. 376, no. 1, p. 55.
5. Lewis, B. and Von Elbe, G., *Combustion, Explosion and Flame in Gases*, New York: Academic, 1987.
6. Korzhavin, A.A., Bunev, V.A., and Babkin, V.S., in *Gaseous and Heterogeneous Detonations: Science to Applications*, Moscow: ENASH, 1999, p. 255.
7. Bunev, V.S. and Zamashchikov, V.V., *Fiz. Goreniya Vzryva*, 2003, vol. 39, no. 5, p. 3.
8. Salgansky, E.A., Polianczuk, E.V., and Manelis, G.B., *Proc. Int. Seminar on Nonequilibrium Processes*, Moscow: Torus, 2005, vol. 1, p. 231.
9. Kislov, V.M., Salgansky, E.A., and Manelis, G.B., *Proc. Int. Seminar on Nonequilibrium Processes*, Moscow: Torus, 2005, vol. 1, p. 247.
10. Gerasimov, G.Ya. and Losev, S.A., *Proc. Int. Seminar on Nonequilibrium Processes*, Moscow: Torus, 2005, vol. 1, p. 30.
11. Kostenko, S.S., Polianczuk, E.V., Karnauch, A.A., Ivanova, A.N., and Manelis, G.B., *Proc. Int. Seminar on Nonequilibrium Processes*, Moscow: Torus, 2005, vol. 1, p. 223.
12. Kostenko, S.S., Polianchik, E.V., Karnaukh, A.A., Ivanova, A.N., and Manelis, G.B., *Khim. Fiz.*, 2006, vol. 25, no. 5, p. 43.
13. Avetisyan, A.A., Azatyan, V.V., Kalachev, V.I., Masalova, V.V., and Piloyan, A.A., *Kinet. Katal.*, 2007, vol. 48, no. 1, p. 1 [*Kinet. Catal.* (Engl. Transl.), vol. 48, no. 1, p. 8].
14. Rubtsov, N.M., Tsvetkov, G.I., and Chernysh, V.I., *Kinet. Katal.*, 1997, vol. 38, no. 4, p. 498 [*Kinet. Catal.* (Engl. Transl.), vol. 38, no. 4, p. 457].
15. Azatyan, V.V., Voevodskii, V.V., and Nalbandyan, A.B., *Kinet. Katal.*, 1961, vol. 2, p. 340.
16. Azatyan, V.V. and Namoradze, M.A., *Fiz. Goreniya Vzryva*, 1974, vol. 10, no. 6, p. 847.
17. Denisov, E.T. and Azatyan, V.V., *Ingibirovanie tsepnykh reaktsii* (Inhibition of Chain Reactions), Chernogolovka, Moscow oblast: Acad. Nauk, 1997.
18. Azatyan, V.V. and Romanovich, L.B., *Izv. Akad. Nauk SSSR, Ser. Khim.*, 1971, no. 5, p. 941.
19. Semenov, N.N., *O nekotorykh problemakh khimicheskoi kinetiki i reaktsionnoi sposobnosti* (Some Problems of Chemical Kinetics and Reactivity), Moscow: Akad. Nauk SSSR, 1958.
20. Azatyan, V.V., Aleksandrov, E.N., and Troshin, A.F., *Kinet. Katal.*, 1975, vol. 16, no. 2, p. 306.
21. DeMore, W.B., Sander, S.P., Golden, D.M., Hampson, R.F., et al., *J. Photochem. Photobiol., A*, 2005, vol. 176, no. 3, p. 129.
22. Germann, T.C. and Miller, W.H., *J. Phys. Chem. A*, 1997, vol. 101, p. 6358.
23. Ryu, S-O., Hwang, S.M., and Rabinovitz, M.J., *Chem. Phys. Lett.*, 1995, vol. 242, p. 279.
24. Biehl, H., Bittner, J., Bohn, B., Stuhl, F., et al., *Int. J. Chem. Kinet.*, 1995, vol. 27, p. 277.
25. Atkinson, R., *Chem. Rev.*, 1986, vol. 86, p. 69.
26. Knox, J.H., *Combust. Flame*, 1965, vol. 9, p. 297.
27. Chapman, S. and Cowling, T.G., *Mathematical Theory of Non-uniform Gases*, Cambridge: Cambridge Univ. Press, 1952.
28. Kokochashvili, T.V., Dzotsenidze, Z.G., Museridze, M.D., Namoradze, M.A., and Azatyan, V.V., *Izv. Akad. Nauk GSSR, Ser. Khim.*, 1979, vol. 5, no. 1, p. 49.
29. Harris, G.W. and Pitts, J.N., *J. Chem. Phys.*, 1982, vol. 77, p. 3994.
30. Tsang, W., *J. Phys. Chem. Ref. Data*, 1990, vol. 19, p. 1.
31. Peters, N. and Rogg, B., *Reduced Kinetic Mechanisms for Applications in Combustion Systems*, Heidelberg: Springer, 1993.
32. Rubtsov, N.M., Tsvetkov, G.I., Chernysh, V.I., and Seplyarsky, B.S., *Mendeleev Commun.*, 2006, p. 282.
33. Hastie, J.W., *J. Res. Natl. Stand. Technol.*, 2001, p. 201.
34. *Khimicheskaya kinetika i tsepnye reaktsii* (Chemical Kinetics and Chain Reactions), Kondrat'ev, V.N., Ed., Moscow: Nauka, 1966.
35. Neiman, M.B. and Egorov, L.N., *Zh. Fiz.Khim.*, 1932, vol. 3, no. 1, p. 61.
36. Rubtsov, N.M., Azatyan, V.V., and Borodulin, R.R., *Izv. Akad. Nauk SSSR, Ser. Khim.*, 1980, no. 6, p. 1234.
37. Linteris, G., *Limits to Effectiveness of Metal-Containing Fire Suppressants: Final Technical Report to SERDP*, Gaithersburg, Md.: National Institute of Standards and Technology, 2004.
38. Rumminger, M.D. and Linteris, G.T., *Combust. Flame*, 2000, vol. 120, p. 451.
39. Azatyan, V.V and Zakhar'in, V.I., *Zh. Fiz. Khim.*, 1977, vol. 51, no. 6, p. 1548.
40. Petrova, L.D., Baratov, A.N., Azatyan, V.V., Kaganova, Z.I., and Makeev, V.I., in *Gorenie i vzryv* (Combustion and Explosion), Moscow: Nauka, 1977, p. 526.